JACS
JOURNAL OF THE AMERICAN CHEMICAL SOCIETY
Article
pubs.acs.org/JACS

Homogeneous Photochemical Water Oxidation by Biuret-Modified Fe-TAML: Evidence of $Fe^{V}(O)$ Intermediate

Chakadola Panda,[†] Joyashish Debgupta,[‡] David Díaz Díaz,[§,∥] Kundan K. Singh,[†] Sayam Sen Gupta,*[,†] and Basab B. Dhar*[,†]

[†]Chemical Engineering and Process Development Division, CSIR-National Chemical Laboratory, Dr. Homi Bhabha Road, Pune 411008, India

[‡]Physical and Materials Chemistry Division, CSIR-National Chemical Laboratory, Dr. Homi Bhabha Road, Pune 411008, India

[§]Institut für Organische Chemie, Fakultät für Chemie und Pharmazie, Universität Regensburg, Universitätsstr. 31, 93053 Regensburg, Germany

[∥]IQAC−CSIC, Jordi Girona 18-26, 08034 Barcelona, Spain

Supporting Information

ABSTRACT: Water splitting, leading to hydrogen and oxygen in a process that mimics natural photosynthesis, is extremely important for devising a sustainable solar energy conversion system. Development of earth-abundant, transition metal-based catalysts that mimic the oxygen-evolving complex of photosystem II, which is involved in oxidation of water to O_2 during natural photosynthesis, represents a major challenge. Further, understanding the exact mechanism, including elucidation of the role of active metal-oxo intermediates during water oxidation (WO), is critical to the development of more efficient catalysts. Herein, we report Fe^{III} complexes of biuret-modified tetra-amidomacrocyclic ligands (Fe-TAML; **1a** and **1b**) that catalyze fast, homogeneous, photochemical WO to give O_2, with moderate efficiency (maximum TON = 220, TOF = 0.76 s^{-1}). Previous studies on photochemical WO using iron complexes resulted in demetalation of the iron complexes with concomitant formation of iron oxide nanoparticles (NPs) that were responsible for WO. Herein, we show for the first time that a high valent $Fe^{V}(O)$ intermediate species is photochemically generated as the active intermediate for the oxidation of water to O_2. To the best of our knowledge, this represents the first example of a molecular iron complex catalyzing photochemical WO through a $Fe^{V}(O)$ intermediate.

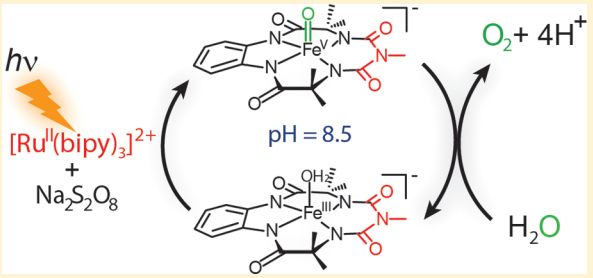

INTRODUCTION

For the past couple of decades, in a quest to develop sustainable energy conversion processes, many chemists around the globe have attempted water splitting using sunlight.[1−3] Water splitting into H_2 and O_2, a multiproton coupled electron transfer (PCET) reaction that is energetically uphill, represents a major technological challenge.[4] Water splitting consists of two processes: water oxidation (WO) or oxygen evolution (OE) and proton reduction.[3] Water oxidation is a greater challenge, as the reaction consists of multielectron transfers and some of them have a high redox potential. WO is of interest also from a biological perspective, because it is one of the crucial steps that occur in the oxygen-evolving complex of photosystem II (OEC-PSII) in green plants and algae, which are responsible for photosynthesis. The oxygen-evolving complex is composed of metal-oxo clusters of earth-abundant manganese[1] and calcium that use sequential cascade reactions to catalyze the four-electron oxidation of water to evolve oxygen (O_2).[5,6]

Seminal developments have taken place in the field of WO catalysis especially with regard to the discovery of a large body of molecular transition-metal complexes and active metal oxide NPs with relatively large turnover numbers (TONs ∼10 000).[7] Most of them involve metal complexes of noble metals (Ru,[7−20] Ir[21−27]), polyoxometalates (POM)[9,28] and metal oxide NPs.[29−33] These homogeneous catalysts have been examined for both chemical oxidation (with a sacrificial oxidant like Ce^{IV}) as well as photochemical oxidation (in the presence of a photosensitizer and sacrificial oxidant like $Na_2S_2O_8$) to oxidize water. For ruthenium (Ru) catalyzed WO, high valent $Ru^{V}(O)$ complexes have been identified as the reactive intermediate responsible for WO.[18,34] However, it is extremely important to develop earth-abundant metal-based catalysts, such as iron (Fe) complexes for WO, since they are expected to be environmentally benign and cheap.[1,35,36] Chemical WO using iron complexes was first reported by Collins, Bernhard, and co-workers using fluorine-substituted Fe−tetra-amidomacrocyclic ligands (Fe-TAML) as a catalyst and Ce^{IV} as the oxidant.[37] Subsequently, Fillol and Costas et al. demonstrated that Fe complexes of tetradentate neutral organic ligands were able to catalyze WO at low pH with TON > 350 and > 1000 using Ce^{IV} and IO_4^-, respectively.[38,39] They demonstrated that

Received: April 18, 2014
Published: August 13, 2014

dx.doi.org/10.1021/ja503753k | J. Am. Chem. Soc. 2014, 136, 12273−12282

a high valent iron oxo species was involved in the formation of the O−O bond. Changes in the steric and electronic property of the liagnds have been made to tune the reactivity of iron complexes.[31,40,41] Meyer and co-workers have proposed the existence of a $Fe^{V}(O)$ species based on electrochemical kinetics (without any spectroscopic characterizations) in electrocatalytic WO that run with lower catalytic efficiency (TONs of 29 over 15 h).[42] Another approach has been recently reported: that of photoelectrochemical WO, by anchoring molecular iron complexes to a solar responsive tungstate.[43] However, the ultimate goal is to develop first-row, transition metal-based systems that catalyze photochemical WO, as sunlight provides the largest renewable energy resource. For first-row transition metals, both cobalt[35,44−46] and manganese[47−49] based molecular complexes, POMs and NPs have been shown to function as efficient catalysts for WO. In contrast, the use of Fe-complexes for photochemical WO is very limited. Very recently, Lau et al. have demonstrated light-driven WO catalyzed by a number of iron complexes and iron salts at pH 7−9 in borate buffer.[29] However, under the reaction conditions, the active species responsible for WO was not a high valent iron oxo complex, but Fe_2O_3 NPs that were formed upon decomposition of the iron complex. Hence, the use of simple iron salts like $Fe(ClO_4)_3$ showed similar catalytic activity, as they also form Fe_2O_3 NPs under reaction conditions. This represents a serious limitation for WO catalyst (WOC) design, since it does not allow researchers to understand fundamental design principles of metal ligand complexes that would make them highly active WOC. Further, understanding the reactive intermediate involved in WO is also critical to development of more efficient WOC. This would allow chemists to understand the electronic properties of the metal complex that can be used to design new WOC with improved activity.

We have recently reported a fifth generation Fe-TAML complex in which the $-CMe_2$ group in the tail part was replaced with a −NMe group.[50,51] This represents a new member of the broad suite of catalysts called TAML activators, which were invented by T. J. Collins in the mid-1990s.[50,52] This biuret-modified Fe-TAML showed improved stability (from pH 1−13) and reactivity toward dye degradation when mediated by H_2O_2 in comparison to the prototype Fe-TAMLs. We have also shown that this ligand framework stabilizes the reactive $Fe^{V}(O)$ in both CH_3CN[53] and CH_3CN-H_2O mixtures.[54] Their high operational stability and ability to stabilize high valent iron oxo species prompted us to explore this biuret-modified Fe-TAML for chemical and photochemical WO. In this paper, we report the chemical and photochemical WO by two biuret-modified Fe-TAML complexes with moderate TONs and yields. The molecularity of the complex remains intact during WO and no formation of iron oxide NP is observed. We also report for the first time photochemical generation of a well-defined high valent $Fe^{V}(O)$ as one of the key intermediates and elucidate its role in WO. Although similar studies showing photochemical formation of a high valent $Fe^{IV}(O)$ have been conducted by Fukuzumi, Nam,[55] Costas[56] and co-workers, photochemical WO has not been explored in any of them. Identification of such $Fe^{V}(O)$ reactive intermediate helps us elucidate the exact mechanism of WO as well as provide insight for designing newer generation WOC based on earth-abundant elements (Scheme 1).

Scheme 1. Homogeneous Photochemical Water Oxidation Using Biuret-Modified Fe-TAML (1a and 1b)

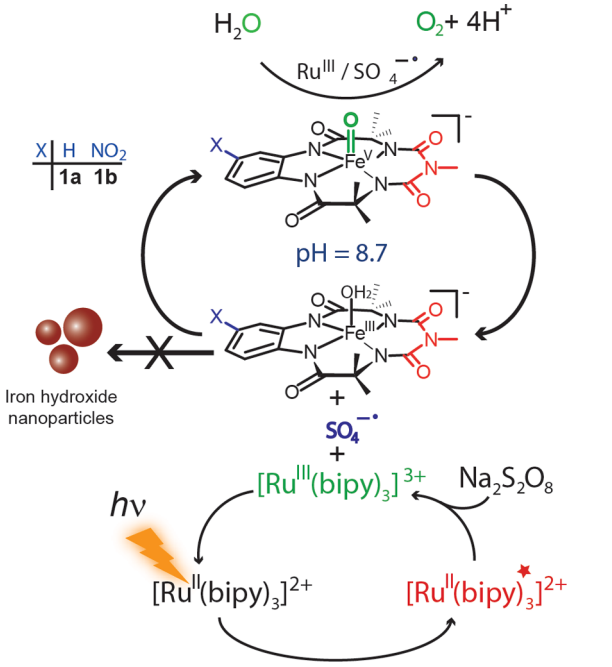

EXPERIMENTAL SECTION

Water Oxidation. *Chemical.* A typical chemical WO was achieved by mixing a solution of **1a** or **1b** (100 μL of a 1.37 mM stock solution in water) with a solution of Cerric Ammonium Nitrate (CAN) (500 μL of a 365 mM stock solution in water) at pH 1 in a sealed vial under stirring at 25 °C. The total reaction volume was kept constant at 600 μL. For kinetic experiments, the catalyst concentration was varied from 0.23 to 0.06 mM. The kinetics of WO was studied by measuring the pressure generated as a result of oxygen evolution with a manometer (Figure S1, Supporting Information (SI)). The differential head space pressure in the manometer was correlated to the amount of oxygen quantified by gas chromatography (GC). The manometer consisted of two sensing ports: one was connected to the reaction vial having both CAN and catalyst and the other one to a reference vial having only CAN solution. As the reaction progressed in the reaction vial, the pressure difference between the reaction and the reference vial increased, which was recorded by the manometer with respect to time. After a certain period of time, the pressure difference in the manometer reached saturation, and hence the oxygen evolution. The evolved oxygen was detected and quantified by GC. Each set of experiments was repeated at least three times to minimize the error associated with it.

Photochemical. In a typical catalytic photochemical WO reaction, 7.4 μM **1a** or **1b** together with 0.83 mM $[Ru(bipy)_3]^{2+}$ and 8.30 mM $Na_2S_2O_8$ in pH 8.7 borate buffer (40 mM) were added such that the total volume of the reaction mixture and head space volume were 4.83 and 3.42 mL respectively. The reaction was initiated by irradiating this mixture with the help of a 3 W blue LED (λ_{max} = 440 nm) at 30 °C (see physical measurements and experimental setup in SI, Figure S2). Each reaction was run for 5 min and the detailed kinetics, identification and quantification of the gaseous products were performed by the same procedure as was done in the case of chemical WO using CAN. Single turnover photochemical WO reactions were carried out at 30 °C in 50% CH_3CN−borate buffer (10 mM; pH 8.7) having 60 μM each of **1a** or **1b**, $[Ru(bipy)_3]^{2+}$ and $Na_2S_2O_8$.

Oxygen Identification and Quantification by GC. After 5 min of catalytic photochemical WO, the excess pressure generated in the reaction vial was released by a Eudiometer[26] setup that displaces approximately 130 μL of water. Similar protocol was also followed for CAN mediated WO. 100 μL of headspace specimen gas was taken by a

dx.doi.org/10.1021/ja503753k | J. Am. Chem. Soc. 2014, 136, 12273−12282

gastight syringe from the reaction vial and injected in to the GC. The head space volume was calculated after 1 h of reaction (assuming completion of reaction) by injecting extra water in to the sealed reaction vial which displaces same amount of water again by the Eudiometer. The total volume (volume displaced due to over pressure as a result of oxygen evolution + headspace volume) was multiplied by the GC quantified oxygen to get the total oxygen evolved in the reaction.[26] The GC was calibrated by using standard oxygen (98%) in a Tedlar bag from Sigma-Aldrich, and this calibration curve was used to quantify the amount of oxygen that evolved from the reaction mixtures. The pressure difference in the manometer for this time period was correlated to the amount of oxygen quantified by GC. Similarly, the quantities of oxygen that evolved for different concentrations of catalyst were calculated and plotted against time.

RESULTS AND DISCUSSION

Physical Properties of Biuret-Modified Fe-TAMLs. Complexes **1a** and **1b** were synthesized (SI) by previously described procedures[51] and characterized using high resolution mass spectrometry (HRMS) (Figure S7 (SI)) and elemental analysis (SI). Both the Fe^{III} complexes (**1a** and **1b**) show an intermediate spin, $S = 3/2$ species in the X-band electron paramagnetic resonance (EPR) at 90 K (Figure S8 (SI)). The cyclic voltammogram (CV) of each complex in CH_3CN using glassy carbon electrode displayed one reversible feature (electrochemical) corresponding to the Fe^{IV}/Fe^{III} couple. This is followed by an electrochemically quasi-reversible couple that probably corresponds to the Fe^{V}/Fe^{IV} couple and an irreversible oxidation peak likely due to a ligand-based oxidation event (Figure S9 (SI), Table 1). When the CV of **1a** and **1b** is performed in water (Figure S10 (SI)), the peaks are poorly resolved due to the pronounced effect of electrochemical double layer. To overcome this issue, we employed the differential pulse voltammetry (DPV) technique. The DPV method, while less sensitive to double layer charging effect, is highly sensitive at low concentrations of the redox species. The results obtained from the DPV method are shown in Figure S11 (SI). The CV of both the complexes **1a** and **1b** in water displayed two electrochemically quasi-reversible couples (Figure S10 (SI)). The variation in formal potentials and kinetics of the redox process of the complexes in acetonitrile and water can be attributed to the differential solvation of the two different solvents (CH_3CN and H_2O). The CVs clearly indicate that it would be possible to generate high-valent iron species in water, which might be an important reactive intermediate for WO.

Table 1. Extinction Coefficient, EPR, Redox Potentials and Acid Stability of 1a and 1b

catalyst	$\varepsilon_{356nm}/M^{-1}$ cm^{-1}	g-values, $S = 3/2$	E_1; E_2/V ($Fe^{IV/III}$; V/IV)	$t_{1/2}$[pH 1]/ sec
1a	3990	3.71, 1.98	0.42; 0.97[a]	2222
1b	9028	4.10, 2.01	0.82; 1.41[a]	7632

[a]In CH_3CN (0.1 M n-Bu_4PF_6) using Glassy carbon working electrode, and the potentials were reported against Ag/AgCl (3 M KCl) reference electrode; scan rate 100 mV/s.

Water Oxidation Using Biuret-Modified Fe-TAML. The high stability of biuret-modified Fe-TAML at extreme pH values, ionic strength and their ability to stabilize high valent iron species in water encouraged us to study their efficacy in both chemical and photochemical WO. For chemical WO, Ce^{IV} was chosen as the sacrificial oxidant, while in photochemical WO the photochemical sensitizer $[Ru(bipy)_3]Cl_2$ and sacrificial oxidant $Na_2S_2O_8$ were used.

Water Oxidation Using CAN at pH 1. CAN is known to be a very strong oxidant ($E_{1/2}$ of $Ce^{IV/III}$ is 1.61 V vs NHE)[57] and is capable of oxidizing a variety of redox-active metal centers in acidic media. Since chemical oxidation by CAN operates at pH 1, it is imperative that the catalyst be stable at such low pH. It is well-known that Fe-TAMLs are in general unstable at acidic pH because they undergo acid-catalyzed demetalation.[58,59] Substitution of $-CF_2$ to the prototypical $-CMe_2$ in the tail part of Fe-TAML has been shown to increase the acid stability several fold.[58,60] Hence, the WO catalysts reported by Collins and Bernarhd have focused on Fe-TAMLs that have a $-CF_2$ group in the tail position.[37] In an earlier paper, we have shown that the introduction of the −NMe in the tail position (biuret-modified Fe-TAML catalyst, **1a**) significantly increases its acid stability ($t_{1/2}$ at pH 1 = 2222 s^{-1}), however they are still susceptible to acid induced

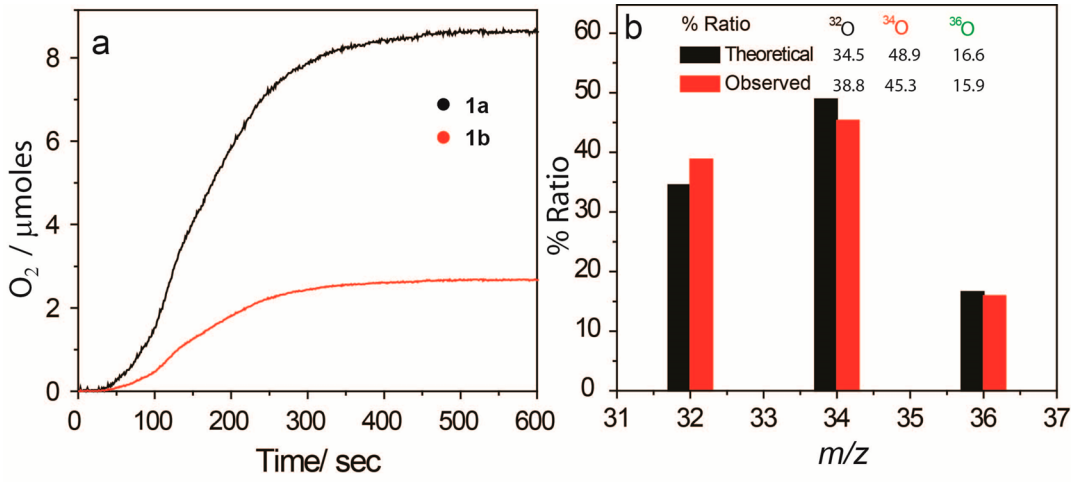

Figure 1. (a) Plot of O_2 formation as a result of photochemical WO by **1a** (black curve) and **1b** (red curve); (b) Comparison for the ratio of ^{32}O, ^{34}O and ^{36}O labeled molecular oxygen evolved (theoretical and observed) during photochemical WO oxidation using 41% $H_2{}^{18}O$ in $H_2{}^{16}O$; Conditions: 3 W blue LED light source; 7.4 μM **1a** or **1b**, 0.83 mM $[Ru(bipy)_3]^{2+}$, and 8.30 mM $Na_2S_2O_8$ in 40 mM borate buffer pH 8.7 at 30 °C; total reaction volume 4.8 mL.

dx.doi.org/10.1021/ja503753k | J. Am. Chem. Soc. 2014, 136, 12273−12282

Table 2. Chemical Yields of O_2 Evolution, Turnover Number (TON) and Turnover Frequency (TOF) for Homogeneous Photochemical WO by 1a, 1b and Some of the Reported First Row Transition Metal Complexes

catalyst (μM)	$[Na_2S_2O_8]$ (mM)	$[Ru(bipy)_3]^{2+}$ (mM)	$[O_2]$ yield (μmol)[a]	TON[b]	TOF (sec^{-1})[b]	chemical yield[c] (%)
1a (7.4)	8.30	0.83	7.86	220 ± 10	0.67	44
1b (7.4)	8.30	0.83	2.44	60 ± 4	0.21	13.4
Mn-L[47] (84)[d]	20	–	0.40	4.20	$\sim 7.9 \times 10^{-4}$	~3.9
Co-POM[44] (5)	5	1	2.50	224	0.25	45
Co-Slp[45] (50)	5	1	8.20	17	0.002	–

[a]Total O_2 yield for a time period of 300 s. [b]TON and TOF for 300 s. [c]Overall chemical yield for a time period of 600 s with respect to $Na_2S_2O_8$ consumption. [d]L = 2,6-bis(4-carboxy-1*H*-benzimidazol-2-yl)-4-methylphenol.

demetalation at low pH.[51] To improve the robustness of biuret-modified Fe-TAMLs under acidic media, an electron withdrawing $-NO_2$ group was introduced in the head aromatic ring of **1a** to make **1b**. Kinetic evaluation of the acid stability of **1b** revealed that the third order dependency (k_3*) was improved by 3 orders of magnitude in comparison to **1a** (explained in SI, Table S1, and Figure S12). This increased stability toward acid catalyzed demetalation of biuret-modified Fe-TAMLs encouraged us to study their efficacy toward WO using Ce^{IV}.

Addition of CAN (305 mM) to a solution of **1a** or **1b** (0.23 mM) at pH 1 leads to the formation of bubbles in the reaction mixture, which indicates the formation of a gaseous product, identified as dioxygen by GC−MS. Subsequently, a manometer was used to measure the pressure generated as a result of oxygen evolution to study the oxygen produced over the course of the reaction. The differential head space pressure in the manometer was correlated to the amount of oxygen evolved quantitatively by GC (Figure S13 (SI)). The plot of initial rates of oxygen evolution for a time period of 50 s as a function of catalyst concentration showed a linear dependency on the catalyst concentration (Figure S13). From this plot, the first order rate constant for WO using **1a** and **1b** was determined to be 0.007 and 0.03 s^{-1}, respectively. The TON over a period of 300 s were calculated to be (10 ± 1) and (17 ± 1) for **1a** and **1b**, respectively, and TOF 0.03 and 0.06 s^{-1}. The TOF values reflect considerably slower reaction rates with respect to the fluorinated Fe-TAML (TOF = 1.3 s^{-1}, TON = 16);[37] however, the overall O_2 yield based on the TONs are very comparable. Also, careful analysis of the evolved gas by GC did not show formation of CO_2, which points to the robust nature of TAML ligand system in oxidizing environments.[52,61]

Photochemical Water Oxidation Using Biuret-Modified Fe-TAML. *1. O_2 Yield and Turnover Number (TON).* In a typical catalytic photochemical WO, oxygen was generated by irradiating a mixture of 7.4 μM **1a** or **1b**, 0.83 mM $[Ru(bipy)_3]^{2+}$ and 8.30 mM $Na_2S_2O_8$ with the use of a 3 W blue LED (λ_{max} = 440 nm) for 10 min in pH 8.7 borate buffer (40 mM). The total amount of O_2 evolved was determined as has been described for chemical WO. It was determined that for catalyst **1a** and **1b** the amount of O_2 generated was 7.86 and 2.44 μmoles respectively over a period of 300 s (Figure 1a). **1a** was shown to have better overall efficiency (TON = 220 ± 10) and O_2 yield (~44%) than **1b** (TON = 60 ± 4, yield ~8.5%), (Table 2), which may be correlated to their differential reactivity toward an electron transfer oxidant (Figure S14 (SI)). The chemical yields were calculated with respect to the consumption of $Na_2S_2O_8$.[44] The evolution of O_2 during photochemical WO reaction using **1a** or **1b** displayed saturation at ~360 s and the pH of the resultant solution dropped from 8.7 to 7.0. As 56% of $Na_2S_2O_8$ was still expected to be remaining in the reaction mixture at the end of 360 s, the saturation observed for O_2 evolution was likely due to proton accumulation in the reaction mixture, which is well-known for most PCET processes.[62] Therefore, we wanted to explore if increasing the pH back to 8.7 would restart the photochemical WO, and attempted to restart the **1a** catalyzed photochemical WO after 360 s by increasing the pH of the mixture from 7.0 to 9.0. Addition of 200 μL of 6 mM aqueous NaOH resulted in resumption of O_2 generation, albeit with lower reaction rates and O_2 formation (~20% of first set) (Figure S15 (SI)). The lower efficiency is likely a result of the reduced amount of $Na_2S_2O_8$ that remained after completion of the first run (i.e., up to 360 s). This experiment indicates that both the catalyst and $Na_2S_2O_8$ are still active even after saturation was observed.

To prove that the oxygen evolved in the above reaction was indeed promoted by catalyst **1a** or **1b**, the following control experiments were performed. Photochemical WO reactions under standard conditions were performed in the absence of (i) photosensitizer, (ii) catalyst **1a** or **1b** and (iii) $Na_2S_2O_8$. The evolution of O_2 was not observed in any of these control experiments. This confirms that all the three components, i.e., catalyst **1a** or **1b**, photosensitizer and $Na_2S_2O_8$, are indeed involved in the catalytic WO process. To prove that the evolved dioxygen was only due to oxidation of water, and not from other sources such as $Na_2S_2O_8$ decomposition, photochemical WO reactions were performed using 41% ^{18}O enriched water under standard operating conditions, as described above. The percentage isotopic ratio distribution of the evolved oxygen for $^{32}O_2$, $^{34}O_2$ and $^{36}O_2$ was 38.8:45.3:15.9 (Figure 1b), which nearly matches the theoretical ratio of 34.5:48.9:16.6 (for experimental details see SI, Figure S16, Table S2). This confirmed that O−O bond formation occurred by the combination of two water molecules during WO process.

2. Biuret-Modified Fe-TAML vs Fe_2O_3 Nanoparticle As Active Catalysts for WO. In a recent paper, Lau et al. demonstrated Fe_2O_3 NPs to be the active catalyst for photochemical WO mediated by iron complexes at basic pH. Studies performed on a series of iron complexes show definitive evidence for ligand dissociation before or after oxidation of the iron complex to generate Fe_2O_3 NPs.[29] We therefore explored the operational stability of **1a** and **1b** in the presence and absence of blue visible light. It is very well established that unlike most other Fe-complexes[29,31] that catalyze WO, Fe-TAMLs display remarkable stability in neutral to basic pH.[63,64] The UV−vis spectral scans of biuret-modified Fe-TAML (**1a**) solution in 40 mM borate buffer (pH 8.7) and 8.30 mM $Na_2S_2O_8$ showed no change in the spectrum over 1 h (Figure S17 (SI)). To evaluate the photochemical stability of **1a**, a solution of 60 μM **1a** and 60 μM $Na_2S_2O_8$ in 40 mM borate buffer pH 8.7 was irradiated for 16 min, and the UV−vis spectrum was recorded. The difference in the absorbance value at the λ_{max} (356 nm/450 nm) before and after irradiation was

dx.doi.org/10.1021/ja503753k | J. Am. Chem. Soc. 2014, 136, 12273−12282

less than 4%. This indicates that the complex is stable under the reaction conditions (Figure S18 (SI)). To probe further, a photochemical WO reaction was initiated with **1a** and the reaction mixture was analyzed by HRMS after completion of the reaction (10 min). HRMS spectrum showed the characteristic peak at m/z = 413.08 for the anion of **1a**, indicating that the complex **1a** was still present after the completion of the reaction (Figure S19 (SI)). In another experiment, O_2 evolution was monitored as a function of increasing concentrations of **1a**. The total amount of O_2 evolved, as well as the initial rates of O_2 production, increased with increase in amount of added **1a** (Figures S20, S21 (SI)). This is in contrast to water oxidation using Fe_2O_3 NPs, in which TONs decrease with increasing concentration of Fe_2O_3 NPs[29] (Figure S21 (SI)). Finally, the reaction mixture was analyzed by both dynamic light scattering (DLS) (Figures S22, S23 (SI)) and transmission electron microscopy (TEM) (Figure S24 (SI)). No evidence of iron oxide NPs was observed in both these studies. All of the above evidence indicates that the active intermediate was based on the biuret-modified Fe-TAML molecule rather than bare iron oxide NPs.

3. Evidence of $Fe^V(O)$ Species As Intermediate in Photochemical WO. Although chemical WO by iron complexes have been shown to proceed through a $Fe^{IV}(O)$ intermediate,[37−39] very little is known about the oxidation states and nuclearity of reactive intermediates involved in photochemical WO by Fe complexes. We hypothesized that the active intermediate for photochemical WO in our case might also be a high valent iron oxo intermediate, as has been recently proposed for Fe-TAML catalyzed chemical WO based on theoretical calculations.[65,66] Very recently, we have demonstrated that the $Fe^V(O)$ intermediate species can be formed with **1a** in CH_3CN−H_2O (v/v) mixture (10% to 90% H_2O) (Figure S25 (SI)).[54] The stability of this $Fe^V(O)$ species decreases with increasing water content and is extremely short-lived in 95% water. This suggested that characterization of such a $Fe^V(O)$ intermediate would be very difficult in 100% H_2O. Additionally, under catalytic conditions used for photocatalytic WO reaction with **1a**, the fast reaction rates together with the presence of excess $[Ru(bipy)_3]^{2+}$ would make it extremely difficult to observe the formation of $Fe^V(O)$ using UV−vis spectroscopy. Hence, we attempted photochemical WO under single turnover conditions using 1 equiv each of catalyst, $Na_2S_2O_8$ and $[Ru(bipy)_3]^{2+}$ in a 50% CH_3CN−buffer mixture. This was expected to reduce the reaction rates, and thus provide us an opportunity to identify and characterize reactive intermediates using spectroscopic techniques. Since such experiments would require the use of mixed solvents, we first carried out the photochemical WO in CH_3CN−buffer to ascertain if O_2 evolution occurred in the presence of such mixed solvent. Photochemical WO in 50% CH_3CN−buffer using 7.4 μM **1a**, 0.83 mM $[Ru(bipy)_3]^{2+}$ and 8.30 mM $Na_2S_2O_8$ showed considerable amount of oxygen evolution with rates considerably slower than that in 100% buffer (Figure S26, Table S3 (SI)). This is expected, because the reactivity of $Fe^V(O)$ is reduced as the CH_3CN content increases. The identification of high valent iron oxo intermediate was thus attempted in CH_3CN−buffer mixture solution using a variety of techniques including HRMS, UV−vis and EPR.

Photochemical WO was performed using equimolar amounts of **1a** or **1b**, $[Ru(bipy)_3]^{2+}$ and $Na_2S_2O_8$ (60 μM each) in 50% CH_3CN−buffer and the reaction mixture was analyzed using HRMS. After 5 min of continuous irradiation, each reaction was diluted 20 times and analysis of the spectrum obtained by HRMS revealed two peaks: one for the unreacted precursor Fe^{III} complex (m/z = 413.08 for **1a** and 458.06 for **1b**) and the other for a $Fe^V(O)$ complex within the instrumental error limit (m/z = 429.07 for **1a** and 474.06 for **1b**) (see Figures 5 and S27 (SI)). Similarly in the presence of 15% $H_2{}^{18}O$, the corresponding $Fe^V(O^{18})$ was observed with m/z value of 431.08 for **1a**, which again confirmed the presence of the $Fe^V(O)$ intermediate (Figure S28 (SI)).

A series of UV−vis experiments were then performed to identify the high valent iron intermediates. An equimolar mixture of $[Ru(bipy)_3]^{2+}$, **1a** and $Na_2S_2O_8$ (60 μM each) was irradiated under dark conditions at 440 nm using the blue LED light source and the progress of the reaction was monitored by UV−vis (Figure 2). Appearance of a new broad peak centered

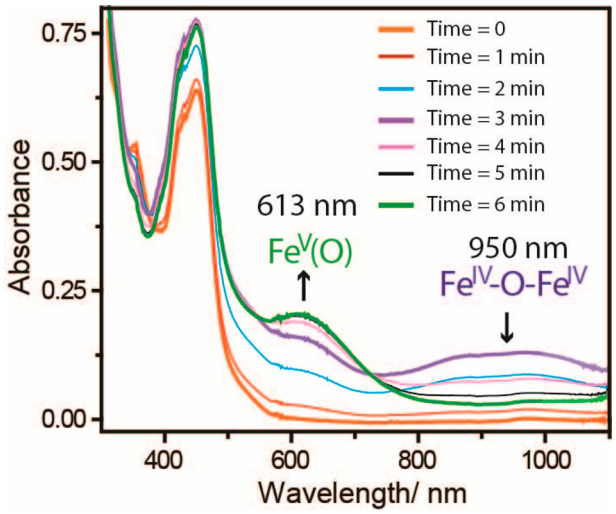

Figure 2. UV−vis spectral scan of a photochemical reaction mixture containing 60 μM each of **1a**, $[Ru(bipy)_3]^{2+}$ and $Na_2S_2O_8$ in 50% CH_3CN−buffer mixture. A broad peak from 800 to 1100 nm after 3 min of reaction (violet spectrum) represents a typical μ-Oxo-Fe^{IV} dimer, while the peak at 613 nm after 6 min (green spectrum) is typical of $Fe^V(O)$ species.

at 950 nm (violet spectrum in Figure 2) was observed during the first 3 min, which then subsequently disappeared with concomitant appearance of another peak at 613 nm (green spectrum in Figure 2) over the next 3 min. The peaks centered at 950 and 613 nm match well with the μ-Oxo-Fe^{IV} dimer (violet spectrum in Figure S29 (SI)) and the $Fe^V(O)$ (green spectrum in Figure S29 (SI)), respectively, which have been independently synthesized using NaOCl and characterized by various techniques.[54] The peak at 450 nm (which initially was due to the presence of $[Ru(bipy)_3]^{2+}$; λ_{max} = 450 nm) increased by 25% (Figure 2) over the course of the reaction (6 min) can be attributed to the formation of μ-Oxo-Fe^{IV} dimer and $Fe^V(O)$ (violet and green spectrum respectively, Figure S29 (SI)). Considering that 80% of unreacted $[Ru(bipy)_3]^{2+}$ was present in the reaction mixture at the end of 3 min, the difference UV−vis spectrum of the reaction mixture after 3 min (violet spectrum, Figure 2) and $[Ru(bipy)_3]^{2+}$ (48 μM, i.e., 80% of starting $[Ru(bipy)_3]^{2+}$; Figure 3b) exactly matches our previously reported diamagnetic μ-Oxo-Fe^{IV} dimer[53] (Figure S30 (SI)). This indicated that irradiation of **1a** with $[Ru(bipy)_3]^{2+}$ and $Na_2S_2O_8$ led to the initial formation of the μ-Oxo-Fe^{IV} dimer. A similar difference spectrum (Figure 3c)

dx.doi.org/10.1021/ja503753k | J. Am. Chem. Soc. 2014, 136, 12273−12282

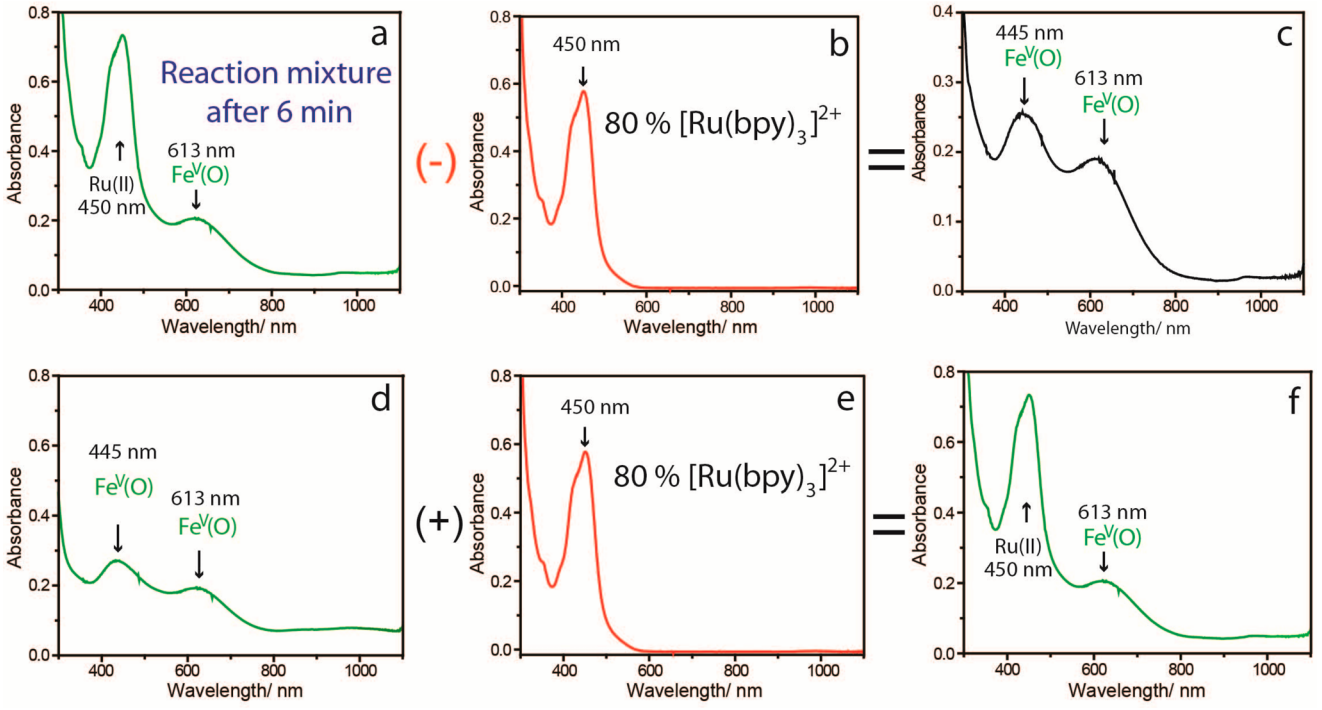

Figure 3. UV−vis spectrum of (a) photochemical reaction mixture after 6 min; (b) $[Ru(bipy)_3]^{2+}$ around 80% (~48 μM) of the amount initially used in the reaction mixture; (c) difference between (a) and (b); (d) well-defined $Fe^V(O)$ formation from **1a** using 1.1 equiv of NaOCl in 50% CH_3CN−buffer mixture; (e) same as (b); (f) addition of (d) and (e) that exactly matches with that of (a).

from the reaction mixture after 6 min exactly matches with that of chemically synthesized $Fe^V(O)$ in 50% CH_3CN−buffer (Figure 3d). To prove further that the spectrum of the reaction mixture was truly due to presence of $Fe^V(O)$ and $[Ru(bipy)_3]^{2+}$, we took the UV−vis spectrum of a mixture of chemically synthesized $Fe^V(O)$ (Figure 3d) and $[Ru(bipy)_3]^{2+}$ (48 μM in 50% CH_3CN−buffer) (Figure 3e). The resultant addition spectrum (Figure 3f) exactly matches with that of the photochemical reaction mixture observed after 6 min (green spectrum, Figure 3a). This again confirmed that the high valent iron species present in the reaction mixture was truly the $Fe^V(O)$. Finally, the $Fe^V(O)$ that was generated photochemically slowly converted to μ-Oxo-Fe^{IV} dimer at room temperature with two clear isosbestic points at 556 and 720 nm, a feature that is characteristic of the spontaneous self-decay of chemically synthesized $Fe^V(O)$ complex of **1a** in CH_3CN[53] or CH_3CN−H_2O mixture (Figure S31 (SI)). On the basis of these observations we propose the initial formation of μ-Oxo-Fe^{IV} dimer (λ_{max} = 950 nm) after 3 min of irradiation followed by slow conversion to the corresponding $Fe^V(O)$ complex.

We then proceeded to prove that the $Fe^V(O)$ intermediate can be regenerated after each cycle to demonstrate the catalytic nature of the reaction. This would also prove that the complex does not decompose under oxidative conditions produced by constant irradiation. First equimolar mixture of **1a**, $[Ru(bipy)_3]^{2+}$ and $Na_2S_2O_8$ (60 μM each) was irradiated for 6 min to generate $Fe^V(O)$ completely (monitored by UV−vis spectroscopy as described before). The irradiation was then stopped and the $Fe^V(O)$ was left to decay (decrease of peak at 613 nm) with concomitant formation of the μ-Oxo-Fe^{IV} dimer (peak at 950 nm). As soon as the μ-Oxo-Fe^{IV} dimer was completely formed, another equivalent of $Na_2S_2O_8$ was added to the reaction mixture and irradiated once again to form $Fe^V(O)$. This procedure was followed up to four cycles to show that $Fe^V(O)$ gets regenerated at the end of each catalytic cycle (Figure 4). Formation of the $Fe^V(O)$ intermediate species was

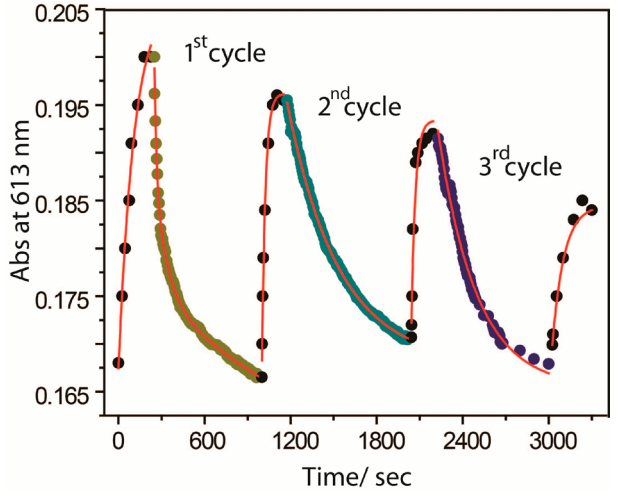

Figure 4. Photochemical regeneration of $Fe^V(O)$ after each catalytic cycle by addition of 1 equiv of $Na_2S_2O_8$ (60 μM) under irradiation to the mixture containing 60 μM each of **1a** and $[Ru(bipy)_3]^{2+}$. Reaction was followed up to four cycles.

further confirmed by X-band EPR measurements of the reaction mixture (Figure 5b). A typical photochemical WO was initiated by addition of **1a** (0.7 mM) with 1 equiv each of $[Ru(bipy)_3]^{2+}$ (0.7 mM) and $Na_2S_2O_8$ (0.7 mM) in a 50% CH_3CN−buffer mixture under continuous irradiation. After 6 min, the formation of a peak characteristic of $Fe^V(O)$ was observed by UV−vis. For EPR analysis at 90 K, the reaction mixture was quenched by freezing in liquid N_2 and absorption peaks at g values of 2.01, 1.98, and 1.76 were observed (Figure

dx.doi.org/10.1021/ja503753k | J. Am. Chem. Soc. 2014, 136, 12273−12282

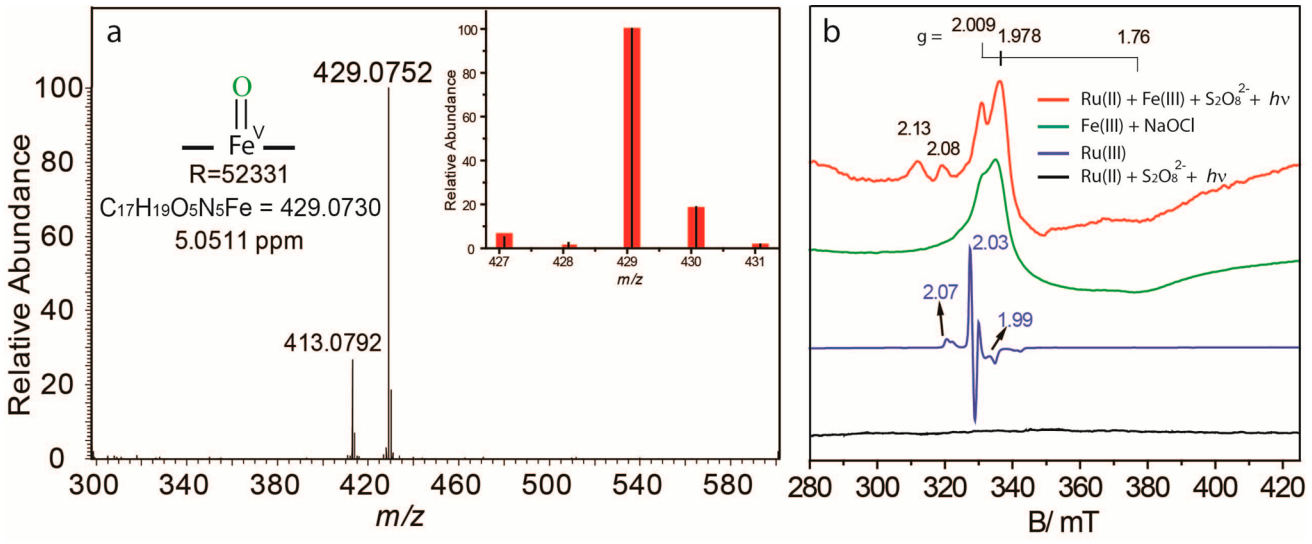

Figure 5. (a) HRMS spectrum of $Fe^{V}(O)$ formed photochemically from **1a** (60 μM) in single turnover experiments using 60 μM each of $[Ru(bipy)_3]^{2+}$ and $Na_2S_2O_8$ in 50% CH_3CN−buffer mixture, Inset shows comparison of simulated (red bars) and observed (black lines) isotopic distribution pattern for ion of interest; (b) X-band EPR spectrum (90 K) of photochemically (red, 0.7 mM each of **1a**, $[Ru(bipy)_3]^{2+}$ and $Na_2S_2O_8$ in 50% CH_3CN−buffer mixture irradiated for 5 min) and chemically (green, using 0.7 mM each of **1a** and NaOCl in 50% CH_3CN−buffer mixture) generated $Fe^{V}(O)$; the blue spectrum corresponds to the chemically synthesized $[Ru(bipy)_3]^{3+}$ (1 mM) and black spectrum for a mixture having 0.7 mM each $[Ru(bipy)_3]^{2+}$ and $Na_2S_2O_8$ in 50% CH_3CN−buffer mixture after irradiation of 5 min.

5b, red). They match very well to our previously reported $Fe^{V}(O)$ intermediate (S = 1/2) prepared by reaction of **1a** with *m*CPBA in CH_3CN.[53] An identical EPR spectrum was also observed by the reaction of 0.70 mM of **1a** and 0.77 mM NaOCl in 50% CH_3CN−buffer (Figure 5b, green). Two additional peaks at g = 2.13 and 2.08 observed in the EPR spectrum of the photochemical reaction mixture probably correspond to some unidentified iron species. As the EPR spectrum of pure $[Ru(bipy)_3]^{3+}$ (also S = 1/2, prepared chemically using reported procedure[67]) have g values 2.07, 2.03, and 1.99 (Figure 5b, blue), the presence of this species in the photochemical reaction mixture is ruled out. Hence, EPR, UV−vis and HRMS studies convincingly show the presence of $Fe^{V}(O)$ as an intermediate for WO.

We then proceeded to investigate the mechanism for the formation of $Fe^{V}(O)$ during the WO reaction. For other transition metal based systems such as ruthenium, it has been proposed that the $[Ru(bipy)_3]^{3+}$ (formed upon oxidation of the $[Ru(bipy)_3]^{2+}$ in the excited state by $Na_2S_2O_8$) oxidizes the molecular WOC which in turn oxidizes water.[12,68] We therefore wanted to explore if addition of preformed $[Ru(bipy)_3]^{3+}$ into a solution of **1a** in 50% CH_3CN−buffer would lead to formation of the $Fe^{V}(O)$. The UV−vis spectrum of a solution containing 60 μM **1a** and 242 mM $[Ru(bipy)_3]^{3+}$ in 50% CH_3CN−buffer at pH 8.7 (violet spectrum, Figure S32 (SI)) showed a spectrum having a broad charge transfer band from 800 to 1100 nm that resembles the well characterized μ-Oxo-Fe^{IV} dimer, the species that is observed after the first 3 min of photochemical WO reaction (violet spectrum, Figure 2). The formation of the dimer is not in agreement with theoretical calculations that predict the formation of $Fe^{IV}(OH)$ species from Fe^{III} aqua complex (**1a**) via PCET in the presence of an electron transfer oxidant.[65,66] However, when the same reaction was performed at pH ∼3 (60 μM **1a**, 242 mM $[Ru(bipy)_3]^{3+}$, 0.5 mM H_2SO_4 in CH_3CN−H_2O), the UV−vis spectrum of the resultant species formed (red spectrum, Figure S32 (SI)) did not match with μ-Oxo-Fe^{IV} dimer. The spectral features of this species resemble a mononuclear Fe^{IV} species of a related Fe-TAML that has recently been proposed by Nam et al.[69] Further, addition of acid to the preformed μ-Oxo-Fe^{IV} dimer converts it into a species whose UV−vis spectral feature is similar to the species that was obtained at pH ∼3 (Figure S33 (SI)). We propose that a mononuclear Fe^{IV} species (likely to be Fe^{IV}−OH) and the μ-Oxo-Fe^{IV} dimer exist in a pH dependent equilibrium with the dimer being the predominant species at pH 8.7. During photochemical WO, Fe^{IV}−OH is first formed by PCET, which is then immediately converted into the μ-Oxo-Fe^{IV} dimer in the reaction medium (pH 8.7).

The mechanism for the formation of $Fe^{V}(O)$ from the μ-Oxo-Fe^{IV} dimer was then investigated. Addition of 4 equiv $[Ru(bipy)_3]^{3+}$ to chemically generated μ-Oxo-Fe^{IV} dimer in 50% CH_3CN−buffer at pH 8.7 did not result in formation of $Fe^{V}(O)$ as was observed by UV−vis. In contrast, addition of 1 equiv of $Na_2S_2O_8$ to the reaction mixture containing **1a** and 4 equiv of $[Ru(bipy)_3]^{3+}$ followed by subsequent irradiation for 3 min resulted in a decrease in the μ-Oxo-Fe^{IV} dimer peak with concomitant increase in the $Fe^{V}(O)$ peak at 613 nm (Figure S34 (SI)). It is therefore suggested that $[Ru(bipy)_3]^{3+}$ was not able to oxidize μ-Oxo-Fe^{IV} dimer to form $Fe^{V}(O)$. Electrochemical studies also support our observation. The second redox peak of **1a** in CH_3CN (expected to be a $Fe^{IV/V}$ couple) has reduction potential close to the $[Ru(bipy)_3]^{II/III}$ couple (∼1.05 V with respect to Ag/AgCl reference electrode (green, Figure S10 (SI)). Hence, addition of excess $[Ru(bipy)_3]^{3+}$ to **1a** does not lead to the formation of $Fe^{V}(O)$. However, we believe that in the presence of $Na_2S_2O_8$, the in situ generated sulfate radical ($SO_4^{\bullet-}$, $E_{1/2}$ = 2.1 V)[70] from the reaction of excited $[Ru(bipy)_3]^{2+}$ and 1 equiv of $Na_2S_2O_8$ most likely oxidizes the μ-Oxo-Fe^{IV} dimer species leading to the formation of $Fe^{V}(O)$.

Role of $Fe^{V}(O)$ in Water Oxidation. Two different pathways may be considered to elucidate the role of $Fe^{V}(O)$ in water oxidation. First, it may be hypothesized that the $Fe^{V}(O)$ species is the real oxidant and is responsible for the generation of O_2. In an alternative scenario, $Fe^{V}(O)$ needs to be

dx.doi.org/10.1021/ja503753k | J. Am. Chem. Soc. 2014, 136, 12273−12282

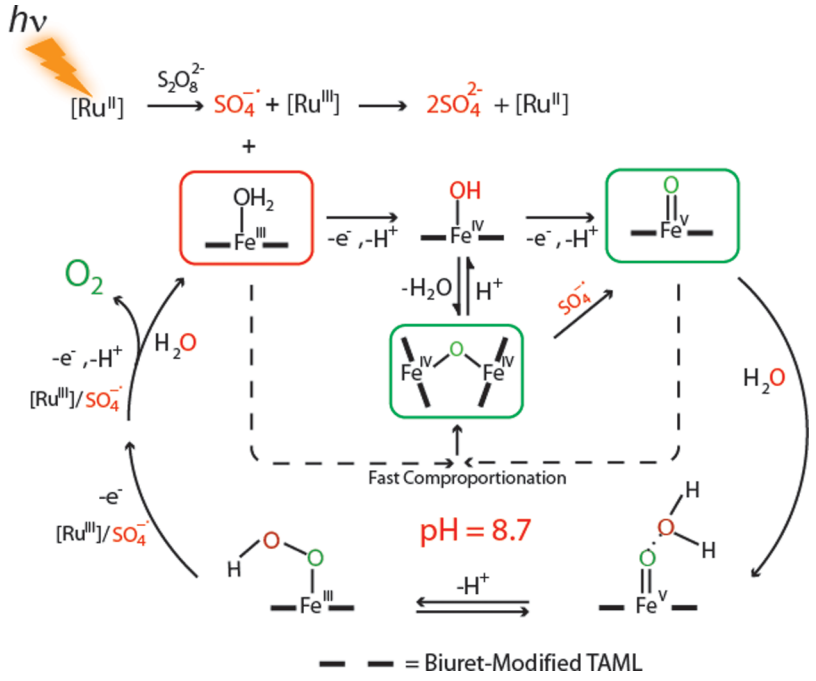

Figure 6. Proposed mechanism of catalytic photochemical WO by biuret-modified Fe-TAML (**1a**). Red box refers to the starting Fe^{III} complex; green boxes indicate intermediates that have been identified and characterized spectroscopically; unboxed intermediates were proposed on the basis of our observations and supported by recently reported theoretical calculations.[65,66]

further oxidized in order to be a water oxidizing species leading to O_2 formation. In an attempt to investigate the role of $Fe^{V}(O)$, we prepared $Fe^{V}(O)$ chemically using **1a** (211 μM) and 1.1 equiv NaOCl in 50% CH_3CN–buffer mixture with rigorous exclusion of O_2. This solution was left to decay over a period of 10 min, and the change in the amount of dissolved O_2 in the reaction mixture was evaluated using a Clark-type electrode (Figure S35 (SI)). In the reaction described above, no change in the amount of dissolved O_2 was detected during the course of the reaction (10 min). This indicates that $Fe^{V}(O)$ species was not the real oxidant for WO leading to O_2 formation (for experimental details, see SI). On the other hand, when the same experiment of $Fe^{V}(O)$ decay was carried out in the presence of 4 equiv of $[Ru(bipy)_3]^{3+}$, 6.5 μM or 0.21 ppm of dissolved oxygen was detected within 2 min of the addition of $[Ru(bipy)_3]^{3+}$ (Figure S35 (SI)). Control experiments that included the addition of $[Ru(bipy)_3]^{3+}$ to (i) **1a**, (ii) μ-Oxo-Fe^{IV} dimer and (iii) NaOCl (231 mM) in 50% CH_3CN–buffer separately did not show any change in dissolved O_2 concentration. We therefore conclude that $Fe^{V}(O)$ itself cannot oxidize water to generate O_2; to act as a WOC, it needs to be further oxidized. The steps that lead to the formation of O_2 from $Fe^{V}(O)$ based on our experimental observation are discussed below.

Proposed Mechanism of Photochemical Water Oxidation. On the basis of our experimental observations and recently reported theoretical calculations for Fe-TAML[65,66] catalyzed chemical WO, we propose the following catalytic cycle for photochemical WO (Figure 6). Irradiation of a mixture of Fe^{III} aqua complex **1a**, $Na_2S_2O_8$ and $[Ru(bipy)_3]^{2+}$ at 440 nm leads to a stepwise formation of $Fe^{IV}(OH)$ first, followed by $Fe^{V}(O)$ via a two-step PCET processes.[62] However, the monoculear Fe(IV) species is not observed as it most likely gets converted into the μ-Oxo-Fe^{IV} dimer (the first intermediate observed experimentally) at the operating pH of 8.7. Formation of μ-Oxo-Fe^{IV} dimer might also arise from fast comproportionation between $Fe^{V}(O)$ and Fe^{III} as has been reported by us before.[53] The $Fe^{V}(O)$ reactive intermediate may then undergo nucleophilic attack by a second water molecule followed by deprotonation and back electron transfer to form the monomeric Fe^{III}-hydroperoxo species. The reaction of $Fe^{V}(O)$ by a cluster of three adjacent water molecules to which proton transfer could occur has been shown to be feasible by DFT studies for a related Fe-complex.[66] The formation of monomeric Fe^{III}-hydroperoxo species has also been proposed by Fillol and Costas from a $Fe^{V}(O)(OH)$ species through a cyclic transition state involving one water molecule. The formation of such species with the oxo and hydroxo group positioned cis to each other is unlikely in our case. In our case, the $Fe^{V}(O)$ species is further oxidized (2 equiv) by the in situ generated oxidants like Ru^{III} and/or $SO_4^{-\bullet}$ to form a likely Fe^{V}-peroxo, which then releases a molecule of oxygen to regenerate the starting aqua Fe^{III} complex (Figure 6). Recently reported theoretical calculations for chemical WO using a related Fe-TAML[65,66] support this proposed mechanism.

■ CONCLUSIONS

Biuret-modified Fe-TAML oxidation catalysts have been synthesized, fully characterized and shown to have high operational stability at extreme pH and under photochemical irradiation in water. The high operational stability and their ability to stabilize high valent iron oxo complexes allowed us to use them as successful catalysts in both chemical (acidic medium) and photochemical (basic medium) WO. During photocatalytic WO, the molecular nature of the biuret-modified Fe-TAML remains intact unlike all other iron complexes that have been studied to date (which are known to decompose to iron oxide NPs). We have also demonstrated for the first time the generation of high valent $Fe^{V}(O)$ intermediate during photochemical irradiation of biuret-modified Fe-TAML with

dx.doi.org/10.1021/ja503753k | J. Am. Chem. Soc. 2014, 136, 12273–12282

$[Ru(bipy)_3]^{2+}$ and $Na_2S_2O_8$. The presence of $Fe^V(O)$ intermediate was supported via EPR, UV−vis and HRMS studies. We propose that the possible nucleophilic attack of water onto $Fe^V(O)$ leads to the formation of a Fe^{III}-hydroperoxo complex, which is then further oxidized, leading to the release of O_2. Although the TONs and yield of O_2 are moderate compared to NP-based systems, this can be significantly improved by the modification of the ligand framework in Fe-TAMLs to minimize the intramolecular self-decay and by heterogenization onto solid support. Efforts in these directions are currently being pursued in our laboratory.

■ ASSOCIATED CONTENT

Supporting Information

Synthesis, characterization of the catalyst (**1b**) using HRMS, FT-IR, UV−vis, EPR, etc., and experimental details of water oxidation. This material is available free of charge via the Internet at http://pubs.acs.org.

■ AUTHOR INFORMATION

Corresponding Authors

ss.sengupta@ncl.res.in
basabbijayi@gmail.com

Notes

The authors declare no competing financial interest.

■ ACKNOWLEDGMENTS

S.S.G. acknowledges DST, New Delhi (EMR/2014/000106) for funding. B.B.D acknowledges DST for funding (Grant No. SERB/F/3945/2013-14) and CSIR for SRA position. C.P, J.D and K.K.S acknowledge CSIR (Delhi) for fellowship. D.D.D thanks DFG for the Heisenberg Professorship Award. Authors thank Prof. Ranjan Das and Dr. Jyotishman Dasgupta for help with EPR measurements at TIFR, Mumbai. Authors also thank Dr. Nandini Devi for GC, Dr. S. K. Asha for UV-vis, Dr. Sanjay P. Borikar (OCD, CSIR-NCL) for GCMS and Soumya Jyoti Chatterjee for DLS measurements at NCL, Pune. Authors thank Mr. Surit Das for editing the manuscript.

■ REFERENCES

(1) Armstrong, F. A. *Philos. Trans. R. Soc., B* **2008**, *363*, 1263.
(2) Ciamician, G. *Science* **1912**, *36*, 385.
(3) McEvoy, J. P.; Brudvig, G. W. *Chem. Rev.* **2006**, *106*, 4455.
(4) Lewis, N. S.; Nocera, D. G. *Proc. Natl. Acad. Sci. U. S. A.* **2006**, *103*, 15729.
(5) Umena, Y.; Kawakami, K.; Shen, J.-R.; Kamiya, N. *Nature* **2011**, *473*, 55.
(6) Yano, J.; Kern, J.; Sauer, K.; Latimer, M. J.; Pushkar, Y.; Biesiadka, J.; Loll, B.; Saenger, W.; Messinger, J.; Zouni, A.; Yachandra, V. K. *Science* **2006**, *314*, 821.
(7) Duan, L.; Bozoglian, F.; Mandal, S.; Stewart, B.; Privalov, T.; Llobet, A.; Sun, L. *Nat. Chem.* **2012**, *4*, 418.
(8) Duan, L.; Araujo, C. M.; Ahlquist, M. S. G.; Sun, L. *Proc. Natl. Acad. Sci. U. S. A.* **2012**, *109*, 15584.
(9) Geletii, Y. V.; Huang, Z.; Hou, Y.; Musaev, D. G.; Lian, T.; Hill, C. L. *J. Am. Chem. Soc.* **2009**, *131*, 7522.
(10) Jiang, Y.; Li, F.; Zhang, B.; Li, X.; Wang, X.; Huang, F.; Sun, L. *Angew. Chem., Int. Ed.* **2013**, *52*, 3398.
(11) Kärkäs, M. D.; Åkermark, T.; Chen, H.; Sun, J.; Åkermark, B. *Angew. Chem., Int. Ed.* **2013**, *52*, 4189.
(12) Kaveevivitchai, N.; Chitta, R.; Zong, R.; El Ojaimi, M.; Thummel, R. P. *J. Am. Chem. Soc.* **2012**, *134*, 10721.
(13) Neudeck, S.; Maji, S.; López, I.; Meyer, S.; Meyer, F.; Llobet, A. *J. Am. Chem. Soc.* **2013**, *136*, 24.
(14) Norris, M. R.; Concepcion, J. J.; Fang, Z.; Templeton, J. L.; Meyer, T. J. *Angew. Chem., Int. Ed.* **2013**, *52*, 13580.
(15) Romain, S.; Bozoglian, F.; Sala, X.; Llobet, A. *J. Am. Chem. Soc.* **2009**, *131*, 2768.
(16) Sala, X.; Maji, S.; Bofill, R.; García-Antón, J.; Escriche, L.; Llobet, A. *Acc. Chem. Res.* **2013**, *47*, 504.
(17) Sala, X.; Romero, I.; Rodríguez, M.; Escriche, L.; Llobet, A. *Angew. Chem., Int. Ed.* **2009**, *48*, 2842.
(18) Tanaka, K.; Isobe, H.; Yamanaka, S.; Yamaguchi, K. *Proc. Natl. Acad. Sci. U. S. A.* **2012**, *109*, 15600.
(19) Tong, L.; Inge, A. K.; Duan, L.; Wang, L.; Zou, X.; Sun, L. *Inorg. Chem.* **2013**, *52*, 2505.
(20) Wang, L.; Duan, L.; Stewart, B.; Pu, M.; Liu, J.; Privalov, T.; Sun, L. *J. Am. Chem. Soc.* **2012**, *134*, 18868.
(21) Cline, E. D.; Adamson, S. E.; Bernhard, S. *Inorg. Chem.* **2008**, *47*, 10378.
(22) Graeupner, J.; Hintermair, U.; Huang, D. L.; Thomsen, J. M.; Takase, M.; Campos, J.; Hashmi, S. M.; Elimelech, M.; Brudvig, G. W.; Crabtree, R. H. *Organometallics* **2013**, *32*, 5384.
(23) Grotjahn, D. B.; Brown, D. B.; Martin, J. K.; Marelius, D. C.; Abadjian, M.-C.; Tran, H. N.; Kalyuzhny, G.; Vecchio, K. S.; Specht, Z. G.; Cortes-Llamas, S. A.; Miranda-Soto, V.; van Niekerk, C.; Moore, C. E.; Rheingold, A. L. *J. Am. Chem. Soc.* **2011**, *133*, 19024.
(24) Hull, J. F.; Balcells, D.; Blakemore, J. D.; Incarvito, C. D.; Eisenstein, O.; Brudvig, G. W.; Crabtree, R. H. *J. Am. Chem. Soc.* **2009**, *131*, 8730.
(25) Lalrempuia, R.; McDaniel, N. D.; Müller-Bunz, H.; Bernhard, S.; Albrecht, M. *Angew. Chem., Int. Ed.* **2010**, *49*, 9765.
(26) McDaniel, N. D.; Coughlin, F. J.; Tinker, L. L.; Bernhard, S. *J. Am. Chem. Soc.* **2007**, *130*, 210.
(27) Parent, A. R.; Brewster, T. P.; De Wolf, W.; Crabtree, R. H.; Brudvig, G. W. *Inorg. Chem.* **2012**, *51*, 6147.
(28) Puntoriero, F.; La Ganga, G.; Sartorel, A.; Carraro, M.; Scorrano, G.; Bonchio, M.; Campagna, S. *Chem. Commun.* **2010**, *46*, 4725.
(29) Chen, G.; Chen, L.; Ng, S.-M.; Man, W.-L.; Lau, T.-C. *Angew. Chem., Int. Ed.* **2013**, *52*, 1789.
(30) Gong, M.; Li, Y.; Wang, H.; Liang, Y.; Wu, J. Z.; Zhou, J.; Wang, J.; Regier, T.; Wei, F.; Dai, H. *J. Am. Chem. Soc.* **2013**, *135*, 8452.
(31) Hong, D.; Mandal, S.; Yamada, Y.; Lee, Y.-M.; Nam, W.; Llobet, A.; Fukuzumi, S. *Inorg. Chem.* **2013**, *52*, 9522.
(32) Hong, D.; Yamada, Y.; Nagatomi, T.; Takai, Y.; Fukuzumi, S. *J. Am. Chem. Soc.* **2012**, *134*, 19572.
(33) Fu, S.; Liu, Y.; Ding, Y.; Du, X.; Song, F.; Xiang, R.; Ma, B. *Chem. Commun.* **2014**, *50*, 2167.
(34) Moonshiram, D.; Alperovich, I.; Concepcion, J. J.; Meyer, T. J.; Pushkar, Y. *Proc. Natl. Acad. Sci. U. S. A.* **2013**, *110*, 3765.
(35) Kanan, M. W.; Nocera, D. G. *Science* **2008**, *321*, 1072.
(36) Singh, A.; Spiccia, L. *Coord. Chem. Rev.* **2013**, *257*, 2607.
(37) Ellis, W. C.; McDaniel, N. D.; Bernhard, S.; Collins, T. J. *J. Am. Chem. Soc.* **2010**, *132*, 10990.
(38) Codolà, Z.; Garcia-Bosch, I.; Acuña-Parés, F.; Prat, I.; Luis, J. M.; Costas, M.; Lloret-Fillol, J. *Chem.—Eur. J.* **2013**, *19*, 8042.
(39) Fillol, J. L.; Codolà, Z.; Garcia-Bosch, I.; Gómez, L.; Pla, J. J.; Costas, M. *Nat. Chem.* **2011**, *3*, 807.
(40) Zhang, B.; Li, F.; Yu, F.; Cui, H.; Zhou, X.; Li, H.; Wang, Y.; Sun, L. *Chem.—Asian J.* **2014**, *9*, 1515.
(41) Hoffert, W. A.; Mock, M. T.; Appel, A. M.; Yang, J. Y.; Eur, J. *Inorg. Chem.* **2013**, *2013*, 3846.
(42) Coggins, M. K.; Zhang, M.-T.; Vannucci, A. K.; Dares, C. J.; Meyer, T. J. *J. Am. Chem. Soc.* **2014**, DOI: 10.1021/ja412822u.
(43) Klepser, B. M.; Bartlett, B. M. *J. Am. Chem. Soc.* **2014**, *136*, 1694.
(44) Huang, Z.; Luo, Z.; Geletii, Y. V.; Vickers, J. W.; Yin, Q.; Wu, D.; Hou, Y.; Ding, Y.; Song, J.; Musaev, D. G.; Hill, C. L.; Lian, T. *J. Am. Chem. Soc.* **2011**, *133*, 2068.
(45) Pizzolato, E.; Natali, M.; Posocco, B.; Montellano Lopez, A.; Bazzan, I.; Di Valentin, M.; Galloni, P.; Conte, V.; Bonchio, M.; Scandola, F.; Sartorel, A. *Chem. Commun.* **2013**, *49*, 9941.

(46) McAlpin, J. G.; Surendranath, Y.; Dincă, M.; Stich, T. A.; Stoian, S. A.; Casey, W. H.; Nocera, D. G.; Britt, R. D. *J. Am. Chem. Soc.* **2010**, *132*, 6882.
(47) Karlsson, E. A.; Lee, B.-L.; Åkermark, T.; Johnston, E. V.; Kärkäs, M. D.; Sun, J.; Hansson, Ö.; Bäckvall, J.-E.; Åkermark, B. *Angew. Chem., Int. Ed.* **2011**, *50*, 11715.
(48) Limburg, J.; Vrettos, J. S.; Liable-Sands, L. M.; Rheingold, A. L.; Crabtree, R. H.; Brudvig, G. W. *Science* **1999**, *283*, 1524.
(49) Robinson, D. M.; Go, Y. B.; Mui, M.; Gardner, G.; Zhang, Z.; Mastrogiovanni, D.; Garfunkel, E.; Li, J.; Greenblatt, M.; Dismukes, G. C. *J. Am. Chem. Soc.* **2013**, *135*, 3494.
(50) Collins, T. J.; Gordon-Wylie, S. W. Long-Lived Homogeneous Oxidation Catalysts, U.S. Patent 5,847,120, December 8, 1998.
(51) Panda, C.; Ghosh, M.; Panda, T.; Banerjee, R.; Sen Gupta, S. *Chem. Commun.* **2011**, *47*, 8016.
(52) Collins, T. J. *Acc. Chem. Res.* **2002**, *35*, 782.
(53) Ghosh, M.; Singh, K. K.; Panda, C.; Weitz, A.; Hendrich, M. P.; Collins, T. J.; Dhar, B. B.; Sen Gupta, S. *J. Am. Chem. Soc.* **2014**, DOI: 10.1021/ja412537m.
(54) Singh, K. K.; Ghosh, M.; Panda, C.; Hendrich, M.; Weitz, A.; Dhar, B.; Sen Gupta, S. (submitted for publication).
(55) Kotani, H.; Suenobu, T.; Lee, Y.-M.; Nam, W.; Fukuzumi, S. *J. Am. Chem. Soc.* **2011**, *133*, 3249.
(56) Company, A.; Sabenya, G.; González-Béjar, M.; Gómez, L.; Clémancey, M.; Blondin, G.; Jasniewski, A. J.; Puri, M.; Browne, W. R.; Latour, J.-M.; Que, L.; Costas, M.; Pérez-Prieto, J.; Lloret-Fillol, J. *J. Am. Chem. Soc.* **2014**, *136*, 4624.
(57) Wadsworth, E.; Duke, F. R.; Goetz, C. A. *Anal. Chem.* **1957**, *29*, 1824.
(58) Ghosh, A.; Ryabov, A. D.; Mayer, S. M.; Horner, D. C.; Prasuhn, D. E.; Sen Gupta, S.; Vuocolo, L.; Culver, C.; Hendrich, M. P.; Rickard, C. E. F.; Norman, R. E.; Horwitz, C. P.; Collins, T. J. *J. Am. Chem. Soc.* **2003**, *125*, 12378.
(59) Polshin, V.; Popescu, D.-L.; Fischer, A.; Chanda, A.; Horner, D. C.; Beach, E. S.; Henry, J.; Qian, Y.-L.; Horwitz, C. P.; Lente, G.; Fabian, I.; Münck, E.; Bominaar, E. L.; Ryabov, A. D.; Collins, T. J. *J. Am. Chem. Soc.* **2008**, *130*, 4497.
(60) Ellis, W. C.; Tran, C. T.; Denardo, M. A.; Fischer, A.; Ryabov, A. D.; Collins, T. J. *J. Am. Chem. Soc.* **2009**, *131*, 18052.
(61) Popescu, D.-L.; Chanda, A.; Stadler, M.; de Oliveira, F. T.; Ryabov, A. D.; Münck, E.; Bominaar, E. L.; Collins, T. J. *Coord. Chem. Rev.* **2008**, *252*, 2050.
(62) Weinberg, D. R.; Gagliardi, C. J.; Hull, J. F.; Murphy, C. F.; Kent, C. A.; Westlake, B. C.; Paul, A.; Ess, D. H.; McCafferty, D. G.; Meyer, T. J. *Chem. Rev.* **2012**, *112*, 4016.
(63) Beach, E. S.; Duran, J. L.; Horwitz, C. P.; Collins, T. J. *Ind. Eng. Chem. Res.* **2009**, *48*, 7072.
(64) Chanda, A.; Shan, X.; Chakrabarti, M.; Ellis, W. C.; Popescu, D. L.; Tiago de Oliveira, F.; Wang, D.; Que, L.; Collins, T. J.; Münck, E.; Bominaar, E. L. *Inorg. Chem.* **2008**, *47*, 3669.
(65) Liao, R.-Z.; Li, X.-C.; Siegbahn, P. E. M. *Eur. J. Inorg. Chem.* **2014**, *2014*, 728.
(66) Ertem, M. Z.; Gagliardi, L.; Cramer, C. J. *Chem. Sci.* **2012**, *3*, 1293.
(67) Shafirovich, V. Y.; Khannanov, N. K.; Shilov, A. E. *J. Inorg. Biochem.* **1981**, *15*, 113.
(68) Duan, L.; Xu, Y.; Zhang, P.; Wang, M.; Sun, L. *Inorg. Chem.* **2009**, *49*, 209.
(69) Kwon, E.; Cho, K.-B.; Hong, S.; Nam, W. *Chem. Commun.* **2014**, *50*, 5572.
(70) Kaledin, A. L.; Huang, Z.; Geletii, Y. V.; Lian, T.; Hill, C. L.; Musaev, D. G. *J. Phys. Chem. A* **2009**, *114*, 73.